Transport of particles in a model of 2D Rayleigh-Benard convection that conserves energy and vorticity

R. Becerril

Instituto de Física y Matemáticas, Universidad Michoacana de San Nicolás de Hidalgo, Edif. C-3, 58040 Morelia, Michoacán, México,
e-mail: ricardo.becerril@umich.mx

M. Maya

Instituto de Física y Matemáticas, Universidad Michoacana de San Nicolás de Hidalgo, Edif. C-3, 58040 Morelia, Michoacán, México,
e-mail: mayav.physicist@gmail.com

Received 9 April 2024; accepted 26 August 2024

In contrast with the Lorenz model for 2-dimensional Rayleigh - Bénard system, the model proposed by Howard - Krishnamurti (HK) allows the possibility of a large scale horizontally shear flow making feasible the study of particles transport. However, this model lacks conservation of energy and vorticity in the absence of forcing and dissipation. A model that incorporates conservation of energy and vorticity was proposed by A. Gluhovsky *et al* (GTA). We perform the linear stability analysis of this later model and study the transport process on this velocity field background and make a comparison with the features of the former model. We found that the basic bifurcation structure is retained by the GTA model and discuss the differences that they indeed have. In regard to the transport processes, the basic features found using the HK velocity field background are also kept by the GTA model. We determine the size of the rather small gap in the Rayleigh number where the transport process shift from being shear flow dominated to a Brownian diffusion process.

Keywords: Convection; Bifurcations; Transport.

DOI: https://doi.org/10.31349/RevMexFis.70.060601

1. Introduction

The study of convection is a long standing field in fluid dynamics [1–4], it certainly plays a central role in a number of important physical processes that occur in our planet, such as the circulation in the atmosphere, which has implications in the climate behavior, in plate tectonics which induce continental motion, the circulation in the oceans, among others. In the astrophysical arena, convection is rather important in the transfer of heat and matter in stars, which in turn significantly affects their activity. Convection also has many industrial applications as in the design of ovens and batteries. It is remarkable that the very basic dynamics of these large convective flows can be experimentally studied with a set-up of much smaller dimensions or studied in a computer. The classical Rayleigh - Bénard (RB) [5, 6] convection is a relatively simple system that has been studied to model some phenomena observed in nature. One of the first attempts to use the RB-system to study climate dynamics was the work by the meteorologist Edward Lorenz [7] in the 1960s, he faced the insurmountable challenge in those years to solve the whole system of equations with the computational limitations of his time. As an alternative, he constructed a dynamical system model from the 2-dimensional RB-system, which consists of an infinite fluid layer of thickness d in a container that is heated from below at temperature T_1 and cooled from above at temperature $T_2 < T_1$, the flat boundaries are perpendicular to gravity $\vec{g}$.

For a 2-dimensional system, it is convenient to introduce the stream function $\psi(x, z, t)$, defined as $\vec{v} = (\partial\psi/\partial z, 0, -\partial\psi/\partial x)$, where $\vec{v}$ is the velocity field of the fluid, in this way, the continuity equation is automatically fulfilled and one is left with only the Navier-Stokes and the diffusion equation. These two equations in the Boussinesq approximation in their non-dimensional form are

$$\frac{\partial}{\partial t}\nabla^2\psi = J(\psi, \nabla^2\psi) + \sigma\nabla^4\psi + \sigma\frac{\partial\theta}{\partial x}, \tag{1}$$

$$\frac{\partial\theta}{\partial t} = J(\psi, \theta) + \frac{\partial\psi}{\partial x}R + \nabla^2\theta, \tag{2}$$

where $\theta(x, z, t)$ is the departure of the linear temperature profile of the conductive state of the fluid layer; hence, it vanishes at the bottom an top of the container. Lorenz employed the stress free boundary conditions for $\psi(x, z, t)$ and $\theta(x, z, t)$ and periodicity in the horizontal direction. The parameters R and σ are the Rayleigh and Prandt numbers defined as

$$R \equiv \frac{gd^3\alpha}{\kappa\nu}\Delta T\,, \qquad \sigma = \frac{\nu}{\sigma}, \tag{3}$$

where g is the acceleration due to gravity, d is the layer depth, α is the thermal expansion coefficient, ν the kinematic viscosity and ΔT the temperature gradient between the top and bottom boundaries of the fluid layer. The Lorenz model belongs to the so called low - order models (LOMs), which are commonly constructed by using the Galerkin method where

the fluid dynamical fields, $\psi(x,z,t)$ and $\theta(x,z,t)$, are expanded in a finite series of an orthonormal function set that satisfies the boundary conditions. A set of ordinary differential equations that governs how the coefficients in this expansion evolves in time is then derived. LOMs contributes to the understanding of the essential dynamics of a system keeping a minimum of modes. Lorenz kept solely three Fourier modes in his model, which has become the iconic example to introduce the concept of chaos in quite a few nonlinear dynamics textbooks. Notwithstanding the attractive features of LOMs, the Galerkin method does not provide a criteria to determine which modes should be retained nor provide the parameter range under which a model closely reflects the behavior of the original system. In this regard, the Howard - Krishnamurti (HK) model [8], provided a model that exhibits the experimentally observed tilting cells of convection, absent in the Lorenz model, this HK model feature allows the possibility of a large scale shear independent of the horizontal coordinate x making feasible the study of passive particle transport, as seen in Binson (1998) [9]. Nevertheless, as other LOMs, the HK model lacks conservation of energy in the absence of forcing and dissipation which in turn may result in trajectories going to infinity as well as may inadequately represent the heat flux. In order to remedy this LOMs deficiency, Thiffeault and Horton [10] added a mode to the temperature expansion. Hermiz [11] had noted that HK model lacked vorticity conservation whose remedy was to add a mode in the stream function expansion. Later on, a model that incorporates conservation of energy and vorticity was proposed by A. Gluhovsky *et al* [12].

Nowadays, numerical algorithms have improved a great deal and parallel computing resources are more available; nonetheless, analysing basic science phenomena and practical engineering systems is still computationally rather expensive, and researchers still find very attractive using LOMs that retain essential features of the original complete equations of motion, thereby reducing notably computational cost in applications that may require a much faster decision making.

The study of kinematics and transport of particles in the fluid system can be performed once the velocity field is obtained. With these LOMs one is able to attain the velocity field $\vec{v}(\vec{x},t)$ in a relatively simple way. Nonetheless, even for simple velocity fields, the trajectories of passive particles may behave randomly, this phenomenon is known as chaotic advection [13]. In this work, we will use the eight mode model that conserves energy and vorticity proposed by A. Gluhovsky *et al* (henceforth we will call it GTA model) to carry out a study of transport of passive particles, that is to say, particles for which $\vec{v}_{\text{particle}} = \vec{v}_{\text{fluid}}$. Once the stream function is known, the trajectories of the passive particles are found by solving the equations

$$\frac{dx}{dt} = \frac{\partial \psi}{\partial z}\,, \qquad \frac{dz}{dt} = -\frac{\partial \psi}{\partial x}. \tag{4}$$

This set of equations resembles the equations of a Hamiltonian system with one degree of freedom, being $\psi(x,z,t)$ the corresponding Hamiltonian. If ψ does not depend on time, particles will simply follow contours with ψ equal to a constant. If ψ is periodic in time, the particles may move in space chaotically. This work will shed light on the differences of using the HK and the GTA models in the study of chaotic advection in large - scale Rayleigh - Bénard convection. We also carry out a bifurcation analysis of the GTA model and compare it with that of the HK model. With this two folded purpose in mind, a brief review of the GTA model is presented in Sec. 2, where we also study its main bifurcation features. The methodology to do the analysis of passive particles transport is exposed in Sec. 3, in this section we also show our numerical results. We end up summarizing our results and making some final remarks in Sec. 5.

2. GTA-model, bifurcation analysis

A. Gluhovsky *et al* modified the HK model of convection with shear in such a way that conserves total energy and total vorticity. They employed the following Galerkin expansion

$$\begin{aligned}
\Psi(x,z,t) &= A(t)\sin(ax)\sin(z) + B(t)\sin(z) \\
&\quad + C(t)\cos(ax)\sin(2z) + G(t)\sin(3z) \\
\theta(x,z,t) &= D(t)\cos(ax)\sin(z) + E(t)\sin(2z) \\
&\quad + F(t)\sin(ax)\sin(2z) + H(t)\sin(4z),
\end{aligned} \tag{5}$$

which satisfies the above mentioned boundary conditions. a is the wave number. The coordinate z was re-scaled so that $0 \leq z \leq \pi$. Inserting this ansatz into the Eqs. (1) y (2) and projecting the resulting equations on the eight modes employed in Eq. (5) the GTA model is readily found

$$\begin{aligned}
\dot{A} &= -\sigma(1+a^2)A + \frac{\sigma a}{1+a^2}D \\
&\quad + \frac{a}{2}\frac{3+a^2}{1+a^2}BC + \frac{3a}{2}\frac{5-a^2}{1+a^2}CG,
\end{aligned} \tag{6}$$

$$\dot{B} = -\sigma B - \frac{3}{4}aAC, \tag{7}$$

$$\begin{aligned}
\dot{C} &= -\sigma(4+a^2)C - \frac{a\sigma}{4+a^2}F \\
&\quad - \frac{a^3}{2(4+a^2)}AB - \frac{3a}{2}\frac{8-a^2}{4+a^2}AG,
\end{aligned} \tag{8}$$

$$\begin{aligned}
\dot{D} &= -(1+a^2)D + RaA - aAE \\
&\quad - \frac{a}{2}BF + \frac{3a}{2}FG,
\end{aligned} \tag{9}$$

$$\dot{E} = -4E + \frac{a}{2}AD, \tag{10}$$

$$\dot{F} = -(4+a^2)F - RaC + \frac{a}{2}BD - \frac{3a}{2}DG + 2aCH, \quad (11)$$

$$\dot{G} = -9\sigma G + \frac{a}{4}AC, \quad (12)$$

$$\dot{H} = -16H - aCF. \quad (13)$$

It has been proven that this dynamical system model $\dot{\vec{X}} = \vec{f}(\vec{X})$ with $\vec{X} = (A, B, C, D, E, F, G, H)$ conserves energy and vorticity (see Ref. [12]). The original HK model is recovered by omitting the last two Eqs. (12) and (13) and setting $G = 0 = H$ in the remaining Eqs. (6) - (11). The Lorenz model is recovered by setting $B = C = G = F = H = 0$ in the above system. The horizontal an vertical components of the fluid velocity field are given by

$$v_x(x,z,t) = \frac{\partial \psi}{\partial z} = A(t)\sin ax\cos z + B(t)\cos z + 2C(t)\cos ax\cos 2z + 3G(t)\cos 3z, \quad (14)$$

$$v_z(x,z,t) = -\frac{\partial \psi}{\partial x} = -aA(t)\cos ax\sin z + aC(t)\sin ax\sin 2z. \quad (15)$$

The Fourier modes with the coefficients $B(t)$ and $G(t)$ appearing in Eq. (14), are the ones that allow long scale flow since they do not depend on the spatial coordinate x. The term with the coefficient $B(t)$ is responsible for the large scale shear flow one has in the lower and upper half of the layer in opposing directions. For the term with the coefficient $G(t)$, the long scale flow is asymmetrical with respect to the plane $z = \pi/2$.

The linearized GTA model around the conductive state represented by the fixed point $\vec{\widetilde{X}} = \vec{0}$ tells us that the components B, E, G and H will definitely decay to zero in time. The other not decaying linearized equations are decoupled in two sets

$$\begin{pmatrix} \dot{A} \\ \dot{D} \end{pmatrix} = \begin{pmatrix} -\sigma(1+a^2) & \frac{\sigma a}{1+a^2} \\ Ra & -(1+a^2) \end{pmatrix} \begin{pmatrix} A \\ D \end{pmatrix},$$

and

$$\begin{pmatrix} \dot{C} \\ \dot{F} \end{pmatrix} = \begin{pmatrix} -\sigma(4+a^2) & -\frac{\sigma a}{4+a^2} \\ -Ra & -(4+a^2) \end{pmatrix} \begin{pmatrix} C \\ F \end{pmatrix}.$$

The first set has its two eigenvalues negative if and only if $R < R_c = (1+a^2)^3/a^2$. The second set has its eigenvalues negative if and only if $R < R_{c2} = (4+a^2)^3/a^2$. The conductive state $\vec{X} = \vec{0}$ is globally stable if $0 < R < R_c$. R_{c2} is the critical Rayleigh number for the modes whose coefficients are C and F. For the case $R > R_{c2}$, in this GTA model, we did not find trajectories going to infinity as it occurs in the HK model which does not conserve energy nor vorticity. As pointed out in Ref. [8], this nonphysical behavior is an artifact of the HK truncation, it does not seem to be present in the GTA model. At any rate, R_{c2} is much larger than the critical Rayleigh number for the onset of steady symmetric cells as well as for the onset of periodic oscillatory motion, and it will not be considered in our study.

As mentioned, for $\widetilde{B} = \widetilde{C} = \widetilde{G} = \widetilde{F} = \widetilde{H} = 0$ the Lorenz model is recovered and there are two fixed points $\vec{\widetilde{X}}_{\pm} = (\widetilde{A}, \widetilde{B}, \widetilde{C}, \widetilde{D}, \widetilde{E}, \widetilde{F}, \widetilde{G}, \widetilde{H})$, where the non vanishing components are given by

$$\widetilde{A} = \pm\frac{2\sqrt{2}}{1+a^2}\sqrt{R-R_c},$$
$$\widetilde{D} = \pm\frac{2\sqrt{2}(1+a^2)}{a}\sqrt{R-R_c},$$
$$\widetilde{E} = R - R_c. \quad (16)$$

These are usually labelled as L_+ and L_-, they constitute symmetric convective cells. By adding a perturbation $\vec{\eta}$ to these fixed points $\vec{\widetilde{X}}_{\pm}$, one carries out linear stability analysis of GTA model and the system splits in two parts. The first part is for the Lorenz variables A, D, E

$$\begin{pmatrix} \dot{\eta}_A \\ \dot{\eta}_D \\ \dot{\eta}_E \end{pmatrix} = \begin{pmatrix} -\sigma(1+a^2) & -\frac{\sigma a}{1+a^2} & 0 \\ -R_c a & -(1+a^2) & -a\widetilde{A} \\ \frac{a}{2}\widetilde{D} & \frac{a}{2}\widetilde{A} & -4 \end{pmatrix} \times \begin{pmatrix} \eta_A \\ \eta_D \\ \eta_E \end{pmatrix} \equiv J_L \vec{\eta_L},$$

whose corresponding polynomial $det\,(J_L - I_{3\times 3}\lambda) = 0$ is a cubic $\lambda^3 + c_2\lambda^2 + c_1\lambda + c_0 = 0$. One has $\lambda = 0$ provided that $c_0 = 0$ which implies $R = R_c$. One encounters the case $\lambda = \pm i\omega_0$ (a Hopf bifurcation) when $c_1 c_2 = c_0$ which leads us to

$$R_H = R_c\frac{\sigma\left(\sigma + 3 + \frac{4}{1+a^2}\right)}{\sigma - 1 - \frac{4}{1+a^2}}, \quad (17)$$

exactly as in the HK model. σ must be larger than $1 + (4/[1+a^2])$ in order that linear instability takes place in the Lorenz coordinates. The second part of the split system for the variables $\vec{\eta}_2 = (B, C, F, G)$ reads $d\vec{\eta}_2^T/dt = J_2\vec{\eta}_2^T$ ($\vec{\eta}_2^T$ stands for transpose of the row vector $\vec{\eta}_2$). The matrix J_2 reads

$$J_2 = \begin{pmatrix} -\sigma & -\frac{3}{4}a\widetilde{A} & 0 & 0 \\ -\frac{a^3}{2}\frac{\widetilde{A}}{4+a^2} & -\sigma(4+a^2) & -\frac{\sigma a}{4+a^2} & -\frac{3a(8-a^2)\widetilde{A}}{4+a^2} \\ \frac{a}{2}\widetilde{D} & -aR & -(4+a^2) & -\frac{3a\widetilde{D}}{2} \\ 0 & \frac{a\widetilde{A}}{2} & 0 & -9\sigma \end{pmatrix}$$

The linearized equation for the perturbation η_H turned out to be $\dot{\eta}_H = -16\eta_H$, it decays and it was simply disregarded. One finds a real eigenvalue of J_2 that changes from being negative to positive at

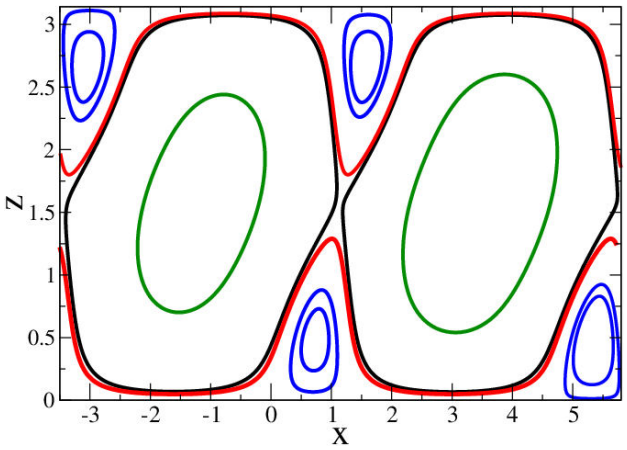

FIGURE 1. Stream lines of steady tilted convective cells are shown in this plot for $R = 44.6$, $\sigma = 1$ and $a = 1.36$. This value is just before the onset of the Hopf bifurcation which takes place at $\widetilde{R} = 44.600433$.

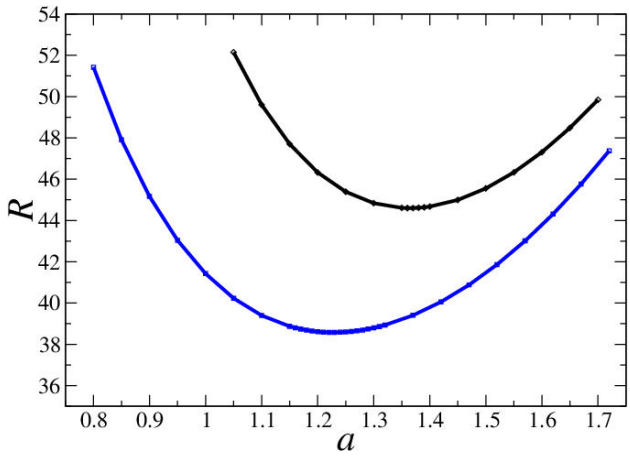

FIGURE 2. Stability diagram for oscillatory flow at $\sigma = 1.0$ for the GTA model (upper curve), the minimum value of the wave number is approximately $a = 1.36$ and $R(1.36) \equiv \tilde{R} \approx 44.600435$. The lower curve represents the onset of oscillatory flow for the HK model.

$$\frac{R^*}{R_C} = \frac{3\frac{(4+a^2)^3}{(1+a^2)^3}\sigma^2 + 11\sigma - 2\frac{(8-a^2)(4+a^2)}{(1+a^2)^2} + 9a^2\frac{(4+a^2)}{(1+a^2)^2}}{3\sigma^2 + 11\sigma - 2\frac{(8-a^2)(4+a^2)}{(1+a^2)^2} + 9a^2\frac{(4+a^2)}{(1+a^2)^2}}. \quad (18)$$

Linear instability occurs on the condition that R^* remains positive, but it might not always be the case. For instance, with $\sigma = 1$ and for all $a > a_c \approx 0.827045$ one gets $R^* > 0$ and the Lorenz fixed point $\vec{X}_L$ becomes unstable at $R = R^*$. For $R > R^*$, tilted convection cells (TC) appear. These tilted cells bifurcate from the Lorenz branches L_+ and L_- and there are two possible angles of tilt of a cell, they are denoted by TC_{++}, TC_{+-}, T_{-+} and TC_{--}, the first sign refers to the Lorenz branches and the second to the two angles of tilt. Figure 1 shows tilted convective cells for $R = 37.0$, $\sigma = 1$ and $a = 1.36$. The upper panel presents counter plot for the current function ψ and the lower panel the velocity plot for the same parameters. This bifurcation to steady tilted cells are present in the HK model but not in the Lorenz model. They are stable in the range $R^* < R < \widetilde{R}$.

The $\widetilde{R}$ marks the onset of a supercritical Hopf bifurcation as the real part of a complex eigenvalue goes from being negative to being positive. Figure 2 presents $\widetilde{R} = \widetilde{R}(a)$ for $\sigma = 1$. The first wave number that becomes unstable is located at the minimum of that curve and it turns out to be $a_c = 1.36$ and $\widetilde{R}(a_c) = 44.6004$. The curve was attained numerically as follows: given a value of a, we solved the GTA dynamical system for a long time, if the system (6)-(13) ended up in a fixed point, we kept increasing in very short steps the value of R until oscillations were observed, and then decreased the value of R and observed whether the system went to a fixed point or oscillated, we followed a kind of a bisection method until a established tolerance was fulfilled; then a was increased by a small quantity and the process was repeated.

At $R = \widetilde{R}$ a stable limit cycle grows out from each of the four tilted branches TC just as in the HK model. Yet the wave numbers values move to the right from $a_{HK} = 1.2$ to $a_{GTA} = 1.36$ and the Rayleigh number of this Hopf bifurcation from $\widetilde{R}_{HK} = 38.802$ (HK - model) to $\widetilde{R}_{GTA} = 44.6004$ (GTA - model). In the upper panel of Fig. 3, we shows an example of these four limit cycles (one in each quadrant) with $\sigma = 1$ and in the variable (A, C) for the Rayleigh number $R = 48 > \widetilde{R} = 44.6004$. As R grows, the cycles in the first and third quadrant widen and then collapse to create just one larger cycle, the same fate follow the cycles in the second and fourth quadrant. This is shown in the lower panel of Fig. 3.

The GTA models which conserve energy and vorticity, preserves basically the same bifurcation structure as the HK model, although the bifurcation points for the tilted cells R^* and the limit cycles $\widetilde{R}$ change as discussed in this section. In the next section, we shall carry out a study of the transport process of passive particles in the GTA model and compare it with the one performed by Bison using the HK model.

3. Transport processes of passive particles

We are interested in velocity fields that are periodic in time in order to perform a study of transport of passive particles. Therefore, we are concerned with the current function $\psi(x, z, t)$ for $R > \widetilde{R}$, we work with $\sigma = 1.0$. We solve the dynamical system (6)-(13) using the Runge Kutta method of order 4 for oscillatory flows together with (4), that is to say, we deal with a 10-dimensional system, eight for the GTA model plus two for the particle coordinates $(x(t), z(t))$. Owing to that we consider the system to be infinite in the horizontal direction, the diffusion of passive particles might be regarded as a 1-dimensional process which is usually characterized by the mean square displacement $\Delta X^2(t)$ (which is time dependent) of a cloud of passive particles released in the convective flow. $\Delta X^2(t)$ is defined as

$$\Delta X^2(t) = \lim_{t\to\infty} < (x - x_0)^2 >, \quad (19)$$

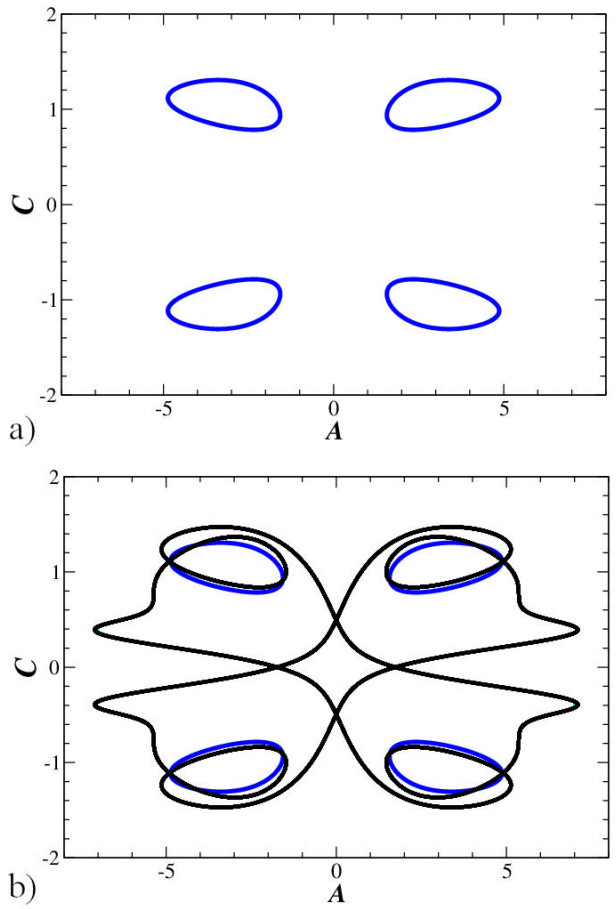

FIGURE 3. We show four limit cycles for $R = 48 > \widetilde{R}$ coming out from the branches $TC_{++}, TC_{+-}, TC_{-+}$ and TC_{--}. For $R = 52 > \widetilde{R}$, the four limit cycles disappear, merging in pairs in two larger cycles (black solid curve and the diamond curve).

where x_0 stands for the initial position of the particle and the brackets $< >$ mean the average of all the particles of a given cloud. It is inferred a relationship of the form

$$\Delta X^2(t) \propto t^m \quad t \to \infty, \tag{20}$$

where m is known as the diffusion exponent. The corresponding diffusion coefficient is defined as

$$D(t) = \frac{\Delta X^2(t)}{2t}. \tag{21}$$

This expression was employed in the first studies of Brownian motion [14,15] for a detailed manner to derived it. For an exponent $m = 1$ the process is referred as Brownian movement where $D(t)$ is actually time independent. For $m = 2$, the diffusion coefficient is proportional to t and the transport process is known as shear flow dominated. There are cases with diffusion exponents between one and two. For $m < 1$ the transport eventually stops. Of course, numerically we work with a finite particles cloud as well as a finite time. In practice, the first step is to run the GTA model for a long transient time to reach the limit cycle. Then, one has to provide a particles cloud, that is to say, a set of initial positions $\{(x_i, z_i)\}_{i=1}^N$ and run the GTA 8-dimensional dynamical system to find $\psi(x, z, t)$ together with (4), namely

$$\frac{dx}{dt} = \frac{\partial \psi}{\partial z}, \qquad \frac{dz}{dt} = -\frac{\partial \psi}{\partial x},$$

for all the $N-$particles. One computes the average $\Delta X^2(t_j)$ for $t_1 < t_2 < ... < t_F$ being t_1 and t_F large enough. Since $\Delta X^2(t) \propto t^m$, by employing the least square method, we fit the data for each given Rayleigh number R to a straight line and the slope would be the diffusion exponent m. We compute m with $N = 5000, 10000$ and 20000; the larger N is, the longer takes our numerical code to finish a computation. The typical difference between $N = 10000$ and $N = 20000$ was typically of order 10^{-3} so we performed most of our calculations with $N = 10000$ and $t_F = 4000$.

Figure 1 constructed with $R = 44.6$, just before the onset of the the Hopf instability, suggests the existence of a pair of saddle points connected by heteroclinic orbits (not shown, but must be rather close to the red trajectories) that separate some core regions of cycles (green and blue closed orbits). As mentioned earlier, there are in the upper and lower sections of the fluid layer large scale shear flows, located between the red curve and the small blue cycles. For this specific example of Fig. 1 ($R = 44.6$), in the upper part ($z > \pi/2$) passive particles move from left to right, and in the lower part ($z < \pi/2$) from right to left. Owing to this large scale flow, with $N = 10000$ passive particles cloud filling a convective cell, for instance, randomly distributed in the spatial domain $\mathcal{D}_\pi \equiv [-\pi/2, \pi/2] \times [0, \pi]$ it is found a diffusion exponent $m = 2.0$. With an initial condition domain located at the middle of the cell $\mathcal{D}_c \equiv [-0.2, 0.2] \times [1.37, 1.57]$ inside a limit cycle, where there had not been inter-cell transport, certainly $m \to 0$ as $t \to 0$. For $R = 44.334 < \widetilde{R}$, we found the same diffusion exponents $m = 2$ or $m = 0$ depending whether the domain $\mathcal{D}_\pi$ or $\mathcal{D}_c$ was used respectively.

We carry out our computations using the domain $\mathcal{D}_\pi$ of N-initial conditions, usually with $N = 10000$, and attain $m = m(R)$. In Fig. 4, we show the behaviour of the diffusion exponent as a function of the relative distance $\epsilon = (R - \widetilde{R})/\widetilde{R}$, relative to the onset of the Hopf bifurcation $\widetilde{R} = 44.600433$, for $\sigma = 1$ and $a = 1.36$. Just before the onset of the Hopf bifurcation ($R < \widetilde{R}$ or equivalently $\epsilon < 0$) $m = 2.0$.

We found that the value of m continues to be equal to two (shear-flow dominated transport process) for $R > \widetilde{R}$ ($\epsilon > 0$) before coming across a small gap of Rayleigh numbers that yield intermediate values $1 < m < 2$ before becoming a Brownian diffusion process $m = 1$. In the upper graph of Fig. 4, we observe a steep variation of m in a very narrow gap in $\epsilon = \epsilon(R)$, the lower graph is a zoom of this narrow gap. This behaviour is also present when the HK model is employed (see [9]). Our theoretical points closely approximate the curve shown in Fig. 4, which was determined by fitting our numerical points to a function of the hyperbolic-tangent, namely $f(x) = 1 + (1 - \tanh(3000x - 1.77))/2$, with an RMS deviation of 0.11.

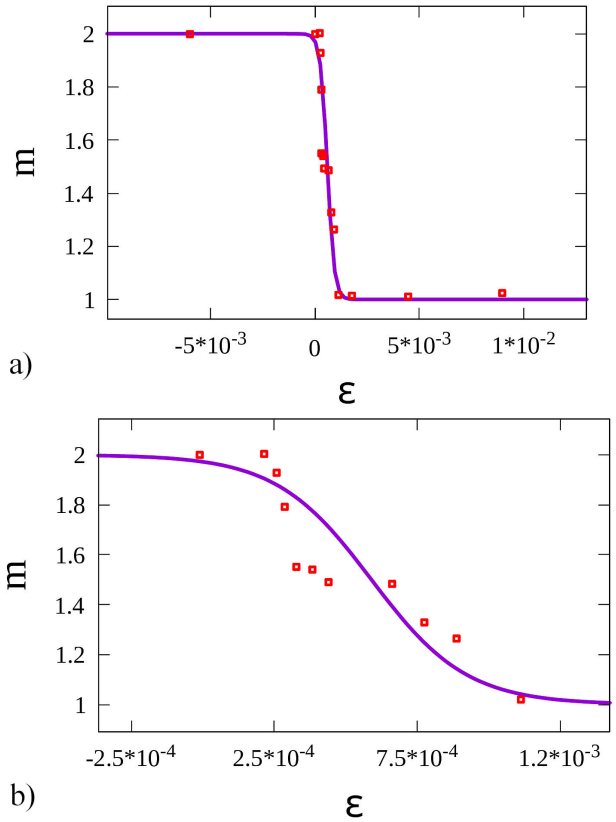

FIGURE 4. Diffusion exponent m as a function of the relative distance $\epsilon = \epsilon(R) = (R - \widetilde{R})/\widetilde{R}$ between a given Rayleigh number R and the onset of Hopf bifurcation located at $\widetilde{R} = 44.600433$, for $\sigma = 1$ and $a = 1.36$. Before the onset of the Hopf bifurcation ($\epsilon < 0$), the exponent $m = 2$. After $\widetilde{R}$ ($\epsilon > 0$), there is a narrow gap where m decreases rapidly to reach unity (Brownian diffusion process).

4. Conclusions and final remarks

We carried out linear stability analysis of the GTA - model which preserves energy and vorticity. The structure of the bifurcation remains fundamentally as the one reported by Ref. [8], with some differences. We enumerate these features next:

- $0 < R \leq R_c$ the conductive state, characterized by $A = B = \ldots H = 0$, is globally stable, any disturbance from this fixed point eventually decays. $R_c = (1 + a^2)^3/a^2$, this expression is the same as in the HK model, as expected.

- $R_c < R \leq R^*$ In this interval, steady symmetric convection cells appear. R^* is given by the Eq. (18) and differs from the expression of the onset of tilted cells for the HK model, the value of a_c where the minimum of the curve $R^*(a)$ is located for the GTA model is slightly higher than the corresponding one for the HK model. Nevertheless for the GTA model R^* is positive only for $a > a_c \approx 0.827045$, which could be an effect of the truncation of this model, for HK, R^* is always positive regardless the value of a.

- $R^* < R \leq \widetilde{R}$ In this interval, tilted convection cells appear, but not predicted by the Lorenz model. Given a value of the Prandtl number, the curve $\widetilde{R} = \widetilde{R}(a)$ can be obtained numerically, this was done for the case where $\sigma = 1$ and is shown in the Fig. 2. As in the case of R^*, the curve of $\widetilde{R}$ moves slightly to the right.

- It seems that the nonphysical trajectories going to infinity are not present in the GTA model.

- In relation to the transport process, the diffusion exponent in the region of the periodic behavior of the velocity field, is monotonically decreasing in R, starting with a shear flow behavior passing through exponents of intermediate value between 1 and 2 to arrive at a behavior of a Brownian process, a behavior shared with the HK model, but shifted to a higher value of R. The gap in R where the system exhibits exponents $m \in (1, 2)$ is rather small as we can see in Fig. 4.

The accuracy of any hydrodynamic model, such as the HK or the GTA, can be determined by analysing the velocity field steaming from the model being studied and comparing it with the one determined by the whole hydrodynamic equations; in our case, also by studying the bifurcation structure and transport processes using the complete hydrodynamic Eqs. (1) and (2), which is certainly computationally much more expensive. This is the subject of another study to be presented somewhere else. Passive particles are an idealized approach, including solute particles that have different mass densities than the mass density of the convective fluid (see [16]) would allow us to see inertia influence on transport processes. This is a study that would be very interesting to carry out in the near future with the velocity field computed from the GTA model.

1. E. Bodenschatz and W. Pesch G. Ahlers, Recent developments in Rayleigh- Bénard convection, *Annu. Rev. Fluid Mech.* **32** (2000) 709, https://doi.org/10.1146/annurev.fluid.32.1.709

2. Y. Fan, Y. Zhao, J. F. Torres, F. Xu, C. Lei, Y. Li and J. Carmeliet, Natural convection over vertical and horizontal heated flat surfaces: A review of recent progress focusing on underpinnings and implications for heat transfer and environmental applications, *Phys. Fluids* **33** (2021) 101301, https://doi.org/10.1063/5.0065125

3. J. J. Song, P. X. Li, L. Chen, C. H. Li, B. W. Li, and L. Y. Huang, A review on Rayleigh-Bénard convection influenced by the complicating factors, *Int. Commun. Heat Mass Transf.* **144** (2023) 106784, https://doi.org/10.1016/j.icheatmasstransfer.2023.106784
4. P. Manneville, Rayleigh-Bénard convection: thirty years of experimental, theoretical, and modeling work, *Springer Tr. Mod. Phys.* **207** (2006) 41, https://doi.org/10.1007/978-0-387-25111-0_3
5. H. Bénard, Étude expérimentale des courants de convection dans une nappe liquide.-Régime permanent: tourbillons cellulaires, *J. Phys. Theor. Appl.* **9** (1900) 513, https://doi.org/10.1051/jphystap:019000090051300
6. L. Rayleigh, On convection currents in a horizontal layer of fluid, when the higher temperature is on the under side, *London Edinburgh Philos. Mag. & J. Sci.* **32** (1916) 529, https://doi.org/10.1080/14786441608635602
7. E. N. Lorenz, Deterministic nonperiodic flow, *J. Atmos. Sci*. **20** (1963) 130, https://doi.org/10.1175/1520-0469(1963)020⟨0130:DNF⟩2.0.CO;2
8. L. N. Howard and R. Krishnamurti, Large-scale flow in turbulent convection: a mathematical model, *J. Fluid Mech.* **170** (1986) 385, https://doi.org/10.1017/S0022112086000940
9. J. Binson, Chaotic advection in large-scale convection, *Int. J. Bifurc. Chaos* **8** (1998) 57, https://doi.org/10.1142/S021812749800005X
10. J. L. Thiffeault and W. Horton, Energy conserving truncations for convection with shear flow, *Phys. Fluids* **8** (1996) 1715, https://doi.org/10.1063/1.868956
11. K. B. Hermiz, P. N. Guzdar and J. M. Finn, Improved low-order model for shear flow driven by Rayleigh-Bénard convection, *Phys. Rev. E.* **51** (1995) 325, https://doi.org/10.1103/PhysRevE.51.325
12. A. Gluhovsky, C. Tong and E. Agee, Selection of modes in convective low-order models, *J. Atmos. Sci.* **59** (2002) 1383, https://doi.org/10.1175/1520-0469(2002)059⟨1383:SOMICL⟩2.0.CO;2
13. H. Aref, Stirring by chaotic advection, *J. Fluid Mech.* **143** (1984) 1, https://doi.org/10.1017/S0022112084001233
14. A. Einstein, Investigations on the Theory of the Brownian Movement(Courier Corporation, U.S.A. 1956) pp. 144, https://store.doverpublications.com/products/9780486603049
15. O. G. Bakunin, Chaotic Flows: correlation effects, transport, and structures, (Springer Science & Business Media, 2011) pp. 354 https://link.springer.com/book/10.1007/978-3-642-20350-3
16. A. Crisanti, M. Falcioni, A. Provenzale, P. Tanga and A. Vulpiani, Dynamics of passively advected impurities in simple two-dimensional flow models, *Phys. Fluids A. Fluid. Dyn.* **4** (1992) 1805, https://doi.org/10.1063/1.858402